

Contribution of Monocarboxylate Transporter 6 to the Pharmacokinetics and Pharmacodynamics of Bumetanide in Mice ¹

 Robert S. Jones,¹ Donna Ruszaj, Mark D. Parker, and  Marilyn E. Morris

Department of Pharmaceutical Sciences, School of Pharmacy and Pharmaceutical Sciences (R.S.J., D.R., M.E.M.) and Department of Physiology and Biophysics, Jacobs School of Medicine and Biomedical Sciences (M.D.P.), University at Buffalo, State University of New York, Buffalo, New York

Received April 7, 2020; accepted June 8, 2020

ABSTRACT

Bumetanide, a sulfamyl loop diuretic, is used for the treatment of edema in association with congestive heart failure. Being a polar, anionic compound at physiologic pH, bumetanide uptake and efflux into different tissues is largely transporter-mediated. Of note, organic anion transporters (SLC22A) have been extensively studied in terms of their importance in transporting bumetanide to its primary site of action in the kidney. The contribution of one of the less-studied bumetanide transporters, monocarboxylate transporter 6 (MCT6; SLC16A5), to bumetanide pharmacokinetics (PK) and pharmacodynamics (PD) has yet to be characterized. The affinity of bumetanide for murine Mct6 was evaluated using Mct6-transfected *Xenopus laevis* oocytes. Furthermore, bumetanide was intravenously and orally administered to wild-type mice (Mct6^{+/+}) and homozygous Mct6 knockout mice (Mct6^{-/-}) to elucidate the contribution of Mct6 to bumetanide PK/PD in vivo. We demonstrated that murine Mct6 transports bumetanide at a similar affinity compared with human MCT6 (78 and 84 μ M, respectively, at pH 7.4). After bumetanide administration, there were no significant differences in plasma PK. Additionally, diuresis

was significantly decreased by ~55% after intravenous bumetanide administration in Mct6^{-/-} mice. Kidney cortex concentrations of bumetanide were decreased, suggesting decreased Mct6-mediated bumetanide transport to its site of action in the kidney. Overall, these results suggest that Mct6 does not play a major role in the plasma PK of bumetanide in mice; however, it significantly contributes to bumetanide's pharmacodynamics due to changes in kidney concentrations.

SIGNIFICANCE STATEMENT

Previous evidence suggested that MCT6 transports bumetanide in vitro; however, no studies to date have evaluated the in vivo contribution of this transporter. In vitro studies indicated that mouse and human MCT6 transport bumetanide with similar affinities. Using Mct6 knockout mice, we demonstrated that murine Mct6 does not play a major role in the plasma pharmacokinetics of bumetanide; however, the pharmacodynamic effect of diuresis was attenuated in the knockout mice, likely because of the decreased bumetanide concentrations in the kidney.

Introduction

Bumetanide is a commonly used, potent loop diuretic for the treatment of congestive heart failure. Its primary mechanism of action is through the inhibition of the sodium-potassium-chloride cotransporter (NKCC), more specifically NKCC2 (SLC12A1), which is expressed in the thick ascending limb of the loop of Henle in the kidney (Lytle et al., 1995; Haas and Forbush, 1998). This electroneutral transporter facilitates the absorption of one sodium, one potassium, and two chloride ions across the plasma membrane, which affects ion homeostasis in both blood and urine. Thus, the major pharmacodynamic effects resulting from the inhibition of this transporter are increased diuresis and

decreased blood pressure due to decreased tubular sodium reabsorption, which can effectively decrease blood pressure. Bumetanide has also been shown to be a selective inhibitor of NKCC1 (SLC12A2), a more ubiquitously expressed isoform that is of recent interest because of its neuronal expression and overexpression in diseases such as neonatal seizures and temporal lobe epilepsy (Blaesse et al., 2009; Kahle et al., 2009; Mao et al., 2012; Puskarjov et al., 2014). Consequently, there are several completed and ongoing clinical trials investigating bumetanide as a treatment of various neurologic disorders (NCT03899324, NCT00830531, NCT03156153).

Considering the popularity of bumetanide as a treatment of heart failure and repurposing for neurologic disorders, the pharmacokinetics of bumetanide have been evaluated using several preclinical rodent models, as well as humans (Holazo et al., 1984; Cook et al., 1988; Han et al., 1993; Weaver et al., 2001; Cleary et al., 2013). Because of the weak acidic nature of the carboxylic acid moiety in bumetanide ($pK_a = 3.6$) (Fig. 1), the compound is negatively charged at physiologic pH, which highlights the contribution of drug transporters to its absorption, distribution, and elimination. In humans, basolateral organic anion

This work was supported by National Institutes of Health National Institute on Drug Abuse [Grant R01-DA023223]. R.S.J. was supported in part by a PhRMA Predoctoral Graduate Fellowship.

¹Current affiliation: Drug Metabolism and Pharmacokinetics, Genentech, Inc., South San Francisco, California.

<https://doi.org/10.1124/dmd.120.000068>.

 This article has supplemental material available at dmd.aspetjournals.org.

ABBREVIATIONS: AUC, area under the curve; CL, clearance; CL_R, renal clearance; cRNA, capped sense RNA; F, bioavailability; f_e, fraction eliminated unchanged in the urine; IS, internal standard; J_{max}, maximum uptake rate; K_t, substrate concentration at the half-maximal uptake rate; LC/MS, liquid chromatography/mass spectrometry; MCT, monocarboxylate transporter; NCA, noncompartmental analysis; NKCC, sodium-potassium-chloride cotransporter; OAT, organic anion transporter; PD, pharmacodynamics; PK, pharmacokinetics.

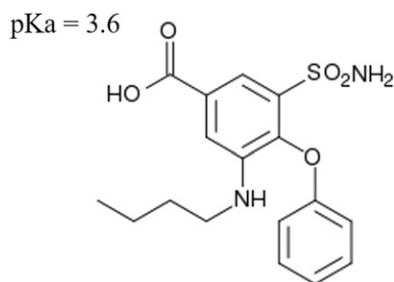


Fig. 1. Chemical structure of bumetanide.

transporter (OAT) 1/3 and apical OAT4 in the kidney have been widely accepted as the major transporters involved in the availability of bumetanide to its NKCC2 site of action (Hasannejad et al., 2004). In addition, bumetanide is primarily eliminated via metabolism, and hepatocyte uptake by hepatic sinusoidal OAT2 is likely to play a major role in its transport into the liver for metabolism (Kobayashi et al., 2005). Less is known about the mechanism of absorption of bumetanide in the intestine; however, absorption has been shown to be rapid because of its onset of action in 30 minutes to 1 hour. Because of the high plasma protein binding of bumetanide (>95%), it is expected that the unbound systemic concentrations are in the low micromolar range after oral and intravenous administration.

There has been interest in investigating the contribution of organic anion transporters because of their importance in moderating tissue-specific concentrations of bumetanide (Murakami et al., 2005; Romermann et al., 2017). One such transporter, monocarboxylate transporter 6 (MCT6, SLC16A5), has been less studied compared with the other bumetanide transporters. Previous evidence suggested that MCT6 is expressed in major tissues related to absorption, distribution, metabolism, and excretion (i.e., kidney, liver, and intestine) and transports a wide variety of substrates similar to that of the OAT solute carrier family, including bumetanide, probenecid, nateglinide, and prostaglandin $F_{2\alpha}$ (Gill et al., 2005; Murakami et al., 2005; Kohyama et al., 2013). Although our laboratory and others have demonstrated that bumetanide is a substrate of human MCT6 (Murakami et al., 2005; Jones et al., 2017), no study has yet investigated the significance of Mct6 in bumetanide transport and its pharmacokinetics (PK)/pharmacodynamics (PD). Therefore, the purpose of this study was to investigate the overall contribution of Mct6 in the PK and PD of bumetanide in mice. Firstly, the *in vitro* transporter kinetic parameters (K_t and J_{max}) were characterized using murine Mct6-transfected *Xenopus laevis* oocytes. Secondly, bumetanide was administered after oral and intravenous administrations to wild-type (Mct6^{+/+}) and Mct6 knockout (Mct6^{-/-}) mice to compare PK parameters (clearance, bioavailability) and a measure of bumetanide pharmacodynamics (24-hour diuresis).

Materials and Methods

Chemicals. Bumetanide ($\geq 98\%$ purity) was purchased from Sigma-Aldrich (St. Louis, MO). All other chemicals and High-performance liquid chromatography-grade reagents were purchased from Fisher Scientific (Hampton, NH). Deuterated bumetanide (bumetanide-d5), used as the internal standard, was purchased from Santa Cruz Biotechnology (Santa Cruz, CA).

Animals. C56BL/6Ncr Mct6^{+/+} wild-type mice (Charles River, Wilmington, MA) and previously generated Mct6^{-/-} knockout mice were used throughout this study (Jones et al., 2019). Body weights throughout the studies ranged from 17 to 35 g, and ages ranged from 8 to 19 weeks old. All mice were housed in cages with a 12-hour light/dark cycle. Animals were given free access to normal chow (Envigo 2018 Teklad global 18% protein extruded rodent diet) ad libitum and water. Experiments were conducted after approval of the Institution of Animal

Use and Care Committee, University at Buffalo. Male mice were used in all studies.

Transfection of Murine Mct6 in *X. laevis* Oocytes. Murine Mct6 was transfected into prepared *X. laevis* oocytes as described previously (Jones et al., 2017; Jones et al., 2020). Briefly, murine Mct6 cRNA was transcribed from *NotI*-linearized pGH19-Mct6 vector using the mMESSAGE mMACHINE T7 transcription kit. Approximately 13.8 nl of cRNA or water was injected into oocytes isolated from digested, resected ovaries the day before. The oocytes were then incubated in OR3 medium at 18°C for 3–5 days for *in vitro* experiments. OR3 medium was prepared as described previously (Musa-Aziz et al., 2010). All cRNA was verified for purity, concentration, stability, and correct size prior to injection.

Bumetanide Uptake Studies. The uptake studies were performed as previously described. Time- and concentration-dependent uptake studies were performed using groups of four to five oocytes in 24-well multidishes, which were preincubated in uptake buffer (15 mM HEPES, 82.5 mM NaCl, 2.5 mM KCl, 1 mM Na₂HPO₄, and 1 mM MgCl₂, adjusted to pH 7.4 with Tris) for 30 minutes. For the time-dependent study, the oocytes were transferred to 400 μ l of uptake buffer containing 0.1 μ M bumetanide, and the oocytes were incubated at pH 7.4 at room temperature (~ 20 – 23°C). For the concentration-dependent study, bumetanide concentrations were varied, and the uptake time was chosen to be in the linear range of the time-dependent study (60 minutes). All uptake was stopped by the addition of ice-cold uptake buffer, and the oocytes were washed three times. Individual oocytes were placed in separate scintillation vials and dissolved in 250 μ l of 10% sodium lauryl sulfate by slowly shaking for 1.5 hours. Radioactivity was determined by liquid scintillation counting after the addition of scintillation cocktail.

Pharmacokinetic and Pharmacodynamic Studies with Bumetanide in Mice. C57BL/6Ncr Mct6^{+/+} and Mct6^{-/-} mice were fasted overnight prior to the experiments and throughout the study. The intravenous and oral doses of bumetanide were chosen to be within a safe and efficacious range to reliably measure the pharmacokinetics (PK) and pharmacodynamics (PD) of the drug. Based on previous experiments in mice and rats (Lee et al., 1994; Kim and Lee, 2001; Brandt et al., 2010; Töpfer et al., 2014), intravenous doses of 1 and 10 mg/kg and oral doses of 2.5 and 25 mg/kg were chosen for this study. No adverse events or toxicity for these doses was reported in the literature, and the LD₅₀ for oral bumetanide administration in mice was reported to be much higher (4.6 g/kg). Similarly to previous studies (Lee et al., 1994; Brandt et al., 2010; Töpfer et al., 2014), bumetanide was dissolved in a small volume of 0.1 N NaOH, diluted with 0.9% saline, and filtered through a 0.45- μ m filter; volumes of 3 ml/kg were used for intravenous injection, and volumes of 8 ml/kg were used for oral administration. Previous studies showed that this dosing formulation did not produce differences in bumetanide PK/PD from other dosing formulations (Lee et al., 1994; Töpfer et al., 2014). Doses were administered as retro-orbital injections for intravenous and via oral gavage for oral doses. Blood was sampled at 5, 15, 30, 45, 60, 120, 240, and 300 minutes postdose via submandibular puncture. Plasma was collected after centrifugation and stored at -80°C until analysis. Urine was collected over a 24-hour period using metabolic cages (Tecniplast, Buguggiate, Italy), and after centrifugation to sediment insoluble material, the volume was measured, and the urine samples were stored at -80°C until analysis. Tissues were collected immediately after cardiac puncture, frozen in liquid nitrogen, and stored at -80°C until analysis.

Plasma and Urine Sample Preparation. Briefly, plasma samples were thawed on ice, and 5 μ l of internal standard (IS: 20 μ g/ml bumetanide-d5) was added to 20 μ l of sample. Protein was precipitated by the addition of 400 μ l of 0.1% formic acid in acetonitrile. The mixture was vortexed, sonicated, and centrifuged at 12,750g at 4°C for 10 minutes to sediment the precipitate. The supernatant (370 μ l) was added to 630 μ l of water in a LC/MS vial, vortexed, and used for analysis. For urine, 5 μ l of IS was added to 50 μ l of sample thawed on ice. Protein was precipitated by the addition of 300 μ l of 0.1% formic acid in acetonitrile. The mixture was vortexed, sonicated, and centrifuged at 12,750g at 4°C for 10 minutes to sediment the precipitate. The supernatant (300 μ l) was added to 300 μ l of water in a LC/MS vial, vortexed, and used for analysis. For urine, $A_{e,24\text{-hour}}$ was calculated by multiplying the concentration of bumetanide by the volume of each urine sample.

Liver and Kidney Sample Preparation. Briefly, whole liver tissue was homogenized in 5:95 v/v methanol/water (5 ml/g). Subsequently, 5 μ l of IS was added to 100 μ l of homogenate. Protein was precipitated by the addition of

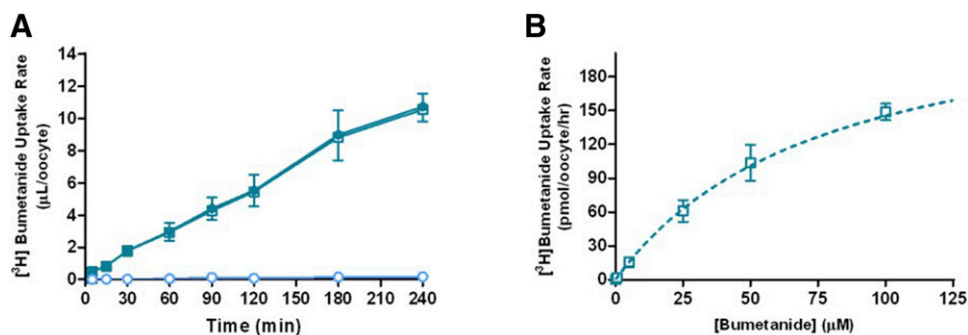


Fig. 2. Time (A) and concentration-dependent (B) uptake of bumetanide in murine Mct6-transfected *X. laevis* oocytes ($N = 4$ to 5 oocytes per data point). Experiment was performed at least three separate times with at least two different ovaries. Data are presented as mean \pm S.D. Closed circles, murine Mct6 cRNA-injected; open circles, water-injected; open squares, Mct6-mediated uptake (Mct6 cRNA-injected minus water-injected). Dashed line represents model fitting using eq. 1 to Mct6-mediated uptake data.

800 μ l of 1% formic acid in acetonitrile. The mixture was vortexed, sonicated, and centrifuged at 12,750g at 4°C for 10 minutes. For the solid-phase extraction, Oasis HLB Prime cartridges were conditioned with 0.5 ml of 1% formic acid in acetonitrile and 0.5 ml of 90:10 acetonitrile/water. For elution, 840 μ l of sample supernatant was loaded onto the column, and the eluent was collected in a clean glass tube. The column was further rinsed two times with 0.5 ml of 90:10 acetonitrile/water, and the eluent was additionally collected. This total eluent was evaporated to dryness under nitrogen, and the sample was reconstituted with 300 μ l of 50:50 acetonitrile/water with vortexing. The final solution was centrifuged at 12,750g at 4°C for 5 minutes to remove insoluble material. The supernatant was transferred to a LC/MS vial for analysis.

Similarly, for kidney cortex samples, the outer layer of a kidney (~40 mg) was collected by sectioning with a razor and prepared in the same manner as liver samples. However, after protein precipitation and sedimentation, 800 μ l of sample supernatant was transferred to a clean glass tube and evaporated to dryness under nitrogen. The sample was reconstituted with 300 μ l of 50:50 acetonitrile/water with vortexing, followed by removal of insoluble material and transfer of the supernatant to a LC/MS vial for analysis.

Liquid Chromatography with Tandem Mass Spectrometry and Chromatographic Conditions. The liquid chromatography with tandem mass spectrometry assay was performed on a Shimadzu Prominence high-performance liquid chromatography instrument with binary pump and autosampler (Shimadzu Scientific, Marlborough, MA) connected to a Sciex API 3000 triple quadrupole tandem mass spectrometer with electrospray ionization (Sciex, Foster City, CA). Chromatographic separation was achieved by injecting 10 μ l of the sample onto a SymmetryShield RP8 (2.1 \times 100 mm, 3.5- μ m particle size; Waters, Milford, MA). Mobile phase A consisted of acetonitrile/water (5:95, v/v) with 0.1% formic acid, and mobile phase B was acetonitrile/water (95:5, v/v) with 0.1% formic acid. The flow rate was 200 μ l/min with a gradient elution profile and a total run time of 13 minutes. The gradient starts at 50% B and increases to 95% over 5 minutes. It was then held at 95% B for 3 minutes before returning to the starting conditions of 50% B. The mass spectrometer was operated in multiple reaction monitoring mode utilizing electrospray ionization for specific detection of bumetanide and bumetanide-d5 as the internal standard. The multiple reaction monitoring transitions monitored were 365.3/240.1 for bumetanide and 370.3/245.2 for the bumetanide-d5. The mass spectrometer parameters were optimized for maximum sensitivity: declustering potential, 38 V; entrance potential, 10 V; collision energy, 22 V; and collision cell exit potential, 20 V. The ion spray voltage was

+5500 V, and the source temperature was 350°C. The data were analyzed using Analyst version 1.4.2 (Sciex).

Assay Validation and Lower Limits of Quantification. The calibration curves for analyzing bumetanide concentrations were linear from 0.0125 to 175 μ g/ml, 0.005 to 70.0 μ g/ml, 5 to 12,500 ng/g, and 10 to 25,000 ng/g for plasma, urine, liver, and kidney tissue, respectively ($R^2 \geq 0.999$). For plasma, the lower limit of quantitation values for bumetanide in these matrices were 0.0125 μ g/ml, 0.005 μ g/ml, 5 ng/g, and 10 ng/g for plasma, urine, liver, and kidney tissue, respectively. LC/MS validations are presented in Supplemental Tables 1–4.

Data Analysis and Statistics. Time-dependent bumetanide uptake rate (microliters per oocyte) was calculated as the ratio of radioactivity in each sample (disintegrations per minute per oocyte) to the initial concentration in the uptake buffer (disintegrations per minute per microliter). All murine Mct6-mediated uptake was calculated as the difference between the murine Mct6 cRNA-injected oocytes and the water-injected oocytes. Data analysis was performed using GraphPad Prism 7 (GraphPad Software Inc., San Diego, CA). The concentration-dependent bumetanide uptake rate (picomoles per oocyte per hour) was calculated as the ratio of radioactivity in each sample (disintegrations per minutes per oocyte) to the concentration in the uptake buffer (disintegrations per minutes per picomole). The kinetic parameters of concentration-dependent uptake of bumetanide was calculated by fitting with the equation below (eq. 1) using weighted nonlinear regression analysis (ADAPT 5; Biomedical Simulations Research, University of South California, Los Angeles, CA):

$$J = \frac{J_{max} \cdot C}{K_t + C} \quad (1)$$

where J is the Mct6-mediated uptake rate, C is the concentration of substrate (micromolar), J_{max} is the maximum uptake rate, and K_t is the substrate concentration at the half-maximal uptake rate (micromolar).

For bumetanide pharmacokinetic parameters, noncompartmental analysis (NCA) was performed in Phoenix WinNonlin 7.0 (Pharsight, Mountain View, CA). Oral bioavailability (F) was calculated using eq. 2:

$$F = \frac{D_{iv} \cdot AUC_{po}}{D_{po} \cdot AUC_{iv}} \quad (2)$$

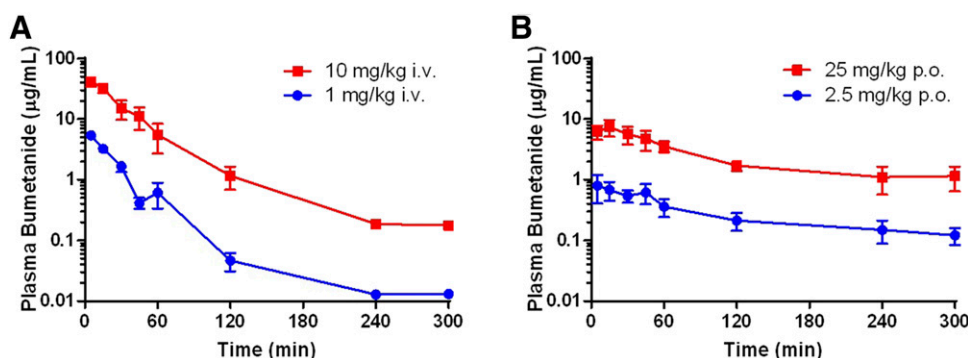


Fig. 3. Concentration-time profiles of bumetanide after intravenous (A) and oral (B) administration in Mct6^{+/+} wild-type mice. $N = 3$ to 4 mice per group. Data are plotted as mean \pm S.D.

TABLE 1
NCA of bumetanide PK in Mct6^{+/+} mice

Data are reported as mean values. For AUC_{0-300 min}, the S.E.M. values are reported in parentheses.

Route	Intravenous		Oral	
	10	1	25	2.5
Dose (mg/kg)				
AUC _{0-300 min} (μg•min/ml)	1.57 × 10 ³ (142)	159 (11.8)	719 (52.2)	82.0 (9.37)
AUC _{0-∞} (μg•min/ml)	1.57 × 10 ³	159	1.16 × 10 ³	122
CL or CL/F ^a (ml/min per kilogram)	6.37	6.28	21.0	20.6
Terminal t _{1/2} (min)	36.2	34.0	284	224
		F	0.295	0.309

t_{1/2}, half-life.

^aCL/F was reported for oral routes of administration.

where *D* is dose and *AUC* is area under the curve from time zero to infinite (AUC_{0-∞}).

For intravenous doses, the fraction eliminated unchanged in the urine (*f_e*) was calculated by dividing A_{e,24-hour} by the dose for each mouse individually and then reported as mean ± S.D. For oral doses, *f_e* was calculated by dividing A_{e,24-hour} by the dose multiplied by *F* for each mouse individually and then reported as mean ± S.D. The observed maximum plasma concentration (*C_{max}*) was also determined after oral administration. Renal clearance (CL_R) was calculated by multiplying total plasma clearance (CL) by *f_e*. Nonrenal clearance was calculated by subtracting CL_R from CL. All statistical analyses were performed using an unpaired Student's *t* test or the one-way unpaired ANOVA followed by Dunnett's test to test for multiple comparisons.

Results

Mct6 Transported Bumetanide at Similar Affinity as Human MCT6. The results from the time- and concentration-dependent uptake of bumetanide for murine Mct6 are presented in Fig. 2. Uptake of 0.1 μM bumetanide at pH 7.4 and room temperature was in the linear range of uptake (Fig. 2A) prior to steady state at approximately 180 minutes. Therefore, for the purpose of the concentration-dependent uptake studies, 60 minutes was used as the uptake time. By fitting with eq. 1, the transporter kinetic parameters (*K_t*, *J_{max}*) for murine Mct6-mediated (Fig. 2B) transport of bumetanide were calculated. At pH 7.4, the affinity (*K_t*) was 77.6 ± 12.6 μM, and the maximal capacity (*J_{max}*) was 258 ± 35.3 picomoles per oocyte per hour.

Plasma Pharmacokinetics of Bumetanide in Wild-type Mct6^{+/+} Mice. After intravenous (1 and 10 mg/kg) and oral (2.5 and 25 mg/kg) administration, bumetanide exhibited apparent biphasic PK (Fig. 3), and no major changes were observed in dose-normalized AUC_{0-∞} estimates from the NCA (Table 1). In addition, there were no changes in CL or *F* at these doses, suggesting that the absorption and elimination of bumetanide at different routes of administration were also linear in mice. The average terminal half-life for bumetanide after intravenous

administration in mice was calculated to be ~35 minutes, which is similar to what was reported in the literature (47 minutes) (Töpfer et al., 2014). After oral administration, although absorption appeared to be rapid (*C_{max}* ≤ 15 minutes), the terminal half-life was much longer compared with that after intravenous administration.

Comparative Plasma Pharmacokinetics of Bumetanide in Mct6^{+/+} and Mct6^{-/-} Mice. To investigate the contribution of Mct6 on the plasma PK of bumetanide, bumetanide was administered at 10 mg/kg i.v. and 25 mg/kg orally to the Mct6^{-/-} and Mct6^{+/+} mice (Fig. 4). For intravenous administration, there were no statistically significant differences between the AUC, CL, or terminal half-life (Table 1). After oral administration, the AUC_{0-300 min} and *C_{max}* both decreased (by 15% and 37%, respectively), although there were no statistically significant differences, likely because of the observed large variability (Table 2).

Urinary Elimination of Bumetanide and Diuresis in Mct6^{+/+} and Mct6^{-/-} Mice. As depicted in Fig. 5, there were no significant differences in the A_{e,24-hour} between the two groups of mice for the highest intravenous and oral doses in the Mct6^{+/+} and Mct6^{-/-} mice (Table 3). CL_R accounted for <25% in all cases, suggesting that the urinary elimination of bumetanide plays a minor role in the total clearance of bumetanide in mice. Upon measuring the volume of urine excreted 24 hours post-dose administration (diuresis) (Fig. 6), there was a significant difference between the Mct6^{-/-} and wild-type Mct6^{+/+} mice after intravenous administration (~55% decrease in Mct6^{-/-} mice).

Impact of Mct6 on Liver and Kidney Concentrations of Bumetanide. To investigate the impact of Mct6 on the exposure of bumetanide to major tissues involved in bumetanide's PK/PD, liver and kidney concentrations of bumetanide were evaluated after oral and intravenous administration, respectively. Figure 7A shows a decrease in liver bumetanide concentrations 60 minutes after an oral dose of 25 mg/kg in the Mct6^{-/-} compared with Mct6^{+/+} mice; however, this

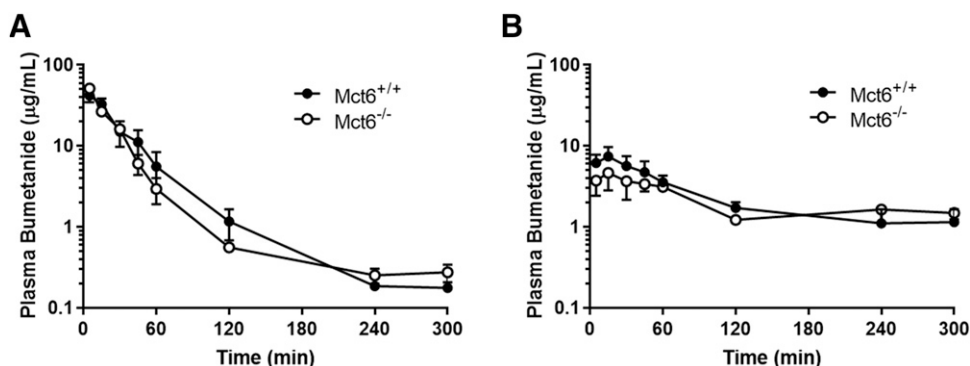


Fig. 4. Concentration-time profiles of bumetanide after 10 mg/kg i.v. (A) and 25 mg/kg oral (B) administration in Mct6^{+/+} (closed symbols) and Mct6^{-/-} (open symbols) mice. *N* = 3 to 4 mice per group. Data are plotted as mean ± S.D.

TABLE 2

NCA of bumetanide PK in Mct6^{+/+} and Mct6^{-/-} mice after 10 mg/kg i.v. and 25 mg/kg oral dose administrationsData are reported as mean values. For AUC_{0-300 min}, the S.E.M. values are reported in parentheses.

Route	Intravenous (10 mg/kg)		Oral (25 mg/kg)	
	Mct6 ^{+/+}	Mct6 ^{-/-}	Mct6 ^{+/+}	Mct6 ^{-/-}
AUC _{0-300 min} (μg•min/ml)	1.57 × 10 ³ (142)	1.45 × 10 ³ (45.3)	719 (52.2)	613 (43.7)
AUC _{0-∞} (μg•min/ml)	1.57 × 10 ³	1.46 × 10 ³	1.16 × 10 ³	1.08 × 10 ³
CL or CL/F ^a (ml/min per kilogram)	6.35	6.84	21.0	22.0
Terminal t _{1/2} (min)	36.2	42.6	284	245
		F	0.295	0.295
		C _{max} (μg/ml)	7.45 (1.15)	4.66 (0.917)

t_{1/2}, half-life.^aCL/F was reported for oral routes of administration.

decrease was not significant ($P = 0.431$). In addition, kidney cortex concentrations of bumetanide, determined 30 minutes after an intravenous dose of 10 mg/kg, exhibited a statistically significant 35% decrease in the Mct6^{-/-} mice compared with Mct6^{+/+} mice (Fig. 7B).

Discussion

In this study, we investigated the contribution of Mct6 to the PK/PD of bumetanide in mice. Previously, Murakami et al. (2005) suggested that Mct6 may play a role in the transport of bumetanide in vivo because of the predicted lack of saturation of human MCT6 at physiologic concentrations of bumetanide. To confirm this in mice, the affinity for murine Mct6 for bumetanide was determined to be 78 μM, which was very similar to what was reported for human MCT6 at physiologic pH (84 μM) (Murakami et al., 2005). Prior to investigating potential changes of bumetanide PK in Mct6^{-/-} mice, bumetanide PK was evaluated in wild-type Mct6^{+/+} mice using two different oral and

intravenous doses. The PK appeared to be biphasic and linear, with no apparent changes in total plasma clearance or bioavailability with changes in dose. The terminal half-life of bumetanide after intravenous administration in mice was similar to what was reported in previous studies in mice (Töpfer et al., 2014; Töllner et al., 2015) (~30–50 minutes). The half-life is somewhat shorter than what is reported for humans (~1 hour) (Dixon et al., 1976). Similar kinetics have been reported in other species, including rat (Lee et al., 1994), dog (Smith and Lau, 1983), and monkey and baboons (Walmsley, 1985), which all demonstrated polyexponential elimination. Additionally, the long terminal half-life after oral administration seen in our data was also demonstrated in baboons, which suggests absorption-limited elimination after oral doses of bumetanide. This phenomenon was also reported in humans (Brater et al., 1984).

Studies of bumetanide PK in Mct6^{-/-} mice indicated that Mct6 does not significantly influence the plasma PK in mice after oral and intravenous administration. Although decreases in C_{max}, AUC, and liver concentrations of bumetanide were observed after oral administration

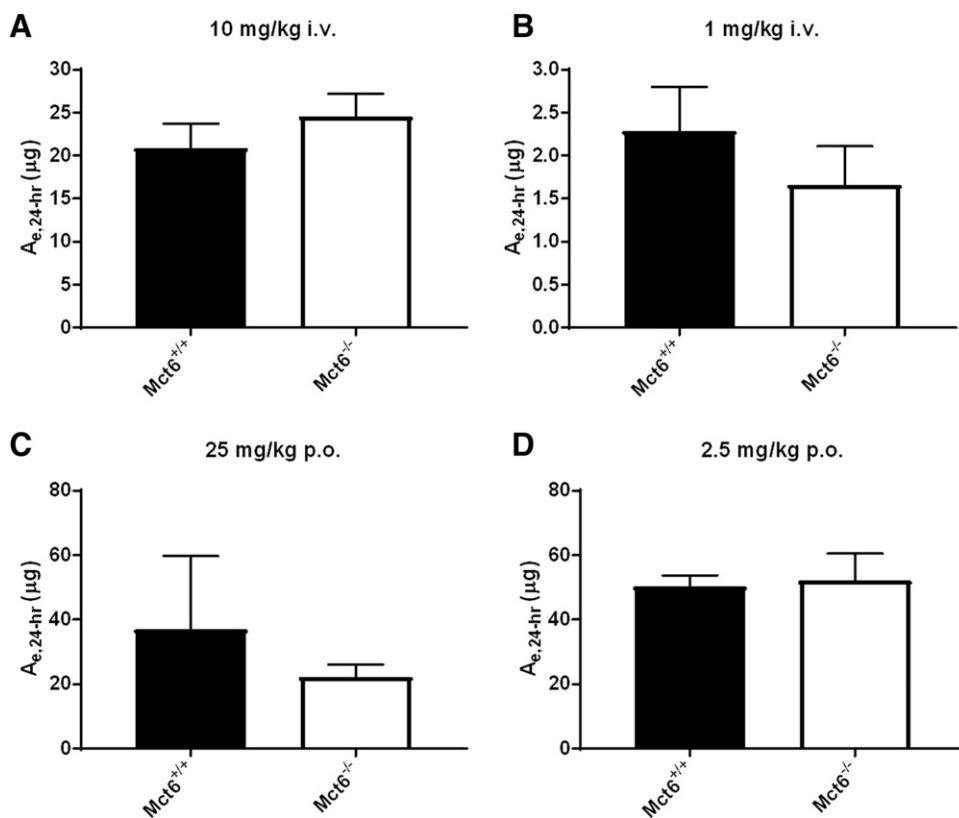


Fig. 5. Amount of bumetanide eliminated unchanged in the urine ($A_{e,24\text{-hr}}$) after different dose administrations [intravenous (A and B); oral (C and D)]. Urine was collected after a 24-hour urine collection. $N = 4$ mice per group. Data are plotted as mean \pm S.D. An unpaired Student's t test was performed to test for statistical significance.

TABLE 3

Summary of clearance parameters in Mct6^{+/+} and Mct6^{-/-} mice after 10 mg/kg i.v. and 25 mg/kg oral dose administrationsData are reported as mean values \pm S.D.

Route	Intravenous (10 mg/kg)		Oral (25 mg/kg)	
	Mct6 ^{+/+}	Mct6 ^{-/-}	Mct6 ^{+/+}	Mct6 ^{-/-}
CL ^a (ml/min per kilogram)	6.35	6.84	6.19	6.48
A _{e,24-h} (μ g)	37.0 (22.8)	22.3 (3.87)	20.9 (2.82)	24.6 (2.62)
f _c	0.101 (0.019)	0.107 (0.007)	0.248 (0.139)	0.145 (0.021)
CL _R (ml/min per kilogram)	0.640 (0.122)	0.730 (0.048)	1.53 (0.857)	0.940 (0.138)
CL _{NR} (ml/min per kilogram)	5.71	6.11	4.66	5.54

CL_{NR}, nonrenal clearance.^aCL for oral administration was calculated as: CL = F · D / AUC_{0-∞}.

in Mct6^{-/-} mice, these changes were not significant. These data suggest that Mct6 may play only a minor role in the first-pass absorption of bumetanide in mice at the doses used in this study. However, further studies are needed prior to drawing these conclusions, partly because of the large variability in the oral PK data. In addition, considering that our AUC_{0-300 min} and AUC_{0-∞} were greater than 40% different after oral administration, further terminal data are required to confirm the terminal plasma concentrations of bumetanide after oral administration.

The diuretic effect of bumetanide was significantly attenuated after intravenous bumetanide administration in Mct6^{-/-} mice compared with wild-type mice; decreased urinary excretion was also observed after oral administration in Mct6^{-/-} mice, but changes were not significant, likely because of the larger variability compared with intravenous administration. Assuming the fraction unbound of bumetanide in mouse plasma is similar to what is estimated in rats (~0.02) (Kim and Lee, 2001), the clearance mediated by renal filtration (CL_{RF}) can be estimated via

glomerular filtration rate [which is estimated to be ~260 μ l/min (Levine et al., 2006)] multiplied by the fraction unbound in plasma. Considering the average weight of a mouse in this study is ~26 g, the CL_{RF} is ~0.21 ml/min per kilogram for bumetanide. Therefore, active renal secretion of bumetanide is a major component of its total renal clearance (which is estimated to be greater than 0.6 ml/min per kilogram). Although renal clearance of bumetanide is not a major route of elimination in mice, it is important to note that its distribution and diuretic effect in the kidney may still be impacted by changes in renal disposition. It is possible that Mct6 plays a role in the secretion of bumetanide into the cortical renal cells, a site of action of bumetanide's inhibition of NKCC2, to exhibit its diuretic effect. This is supported by the fact that bumetanide concentrations in kidney cortex were significantly decreased in Mct6^{-/-} mice after an intravenous dose of 10 mg/kg at 30 minutes postadministration. However, further kidney concentration data, as well as the evaluation of changes in other determinants of

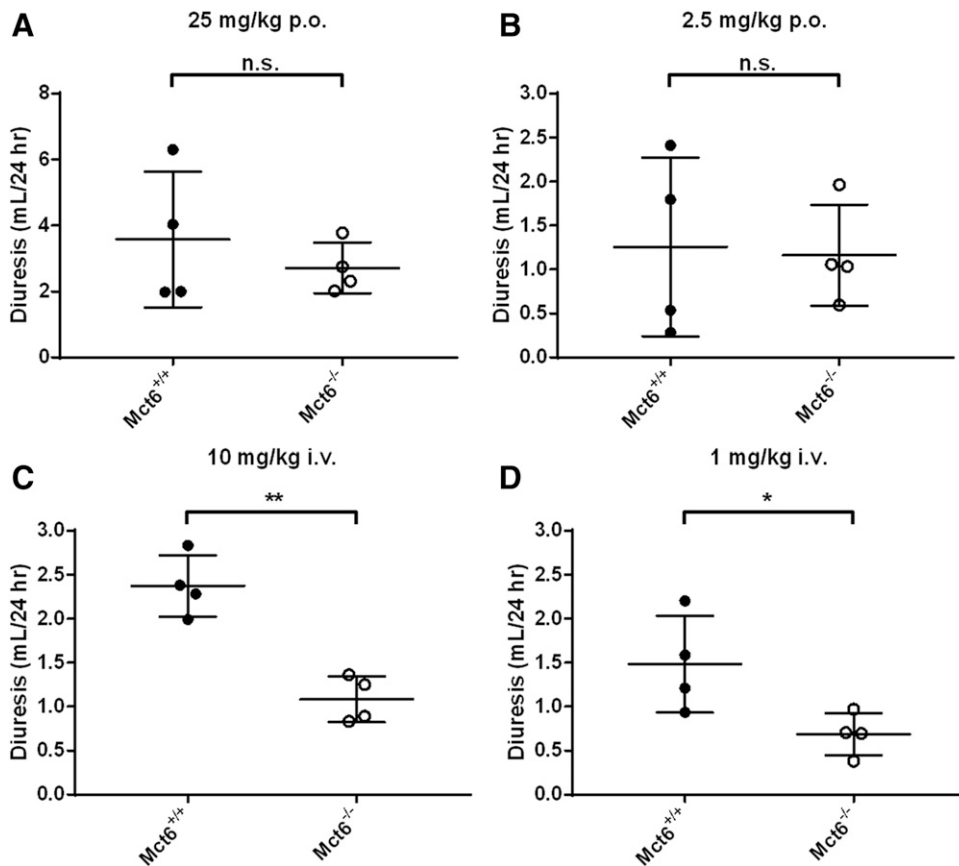


Fig. 6. Urinary output after administration of bumetanide in Mct6^{+/+} and Mct6^{-/-} mice after doses of 25 mg/kg orally (A), 2.5 mg/kg orally (B), 10 mg/kg i.v. (C) and 1 mg/kg i.v. (D). *N* = 4 mice per group. Data are plotted as mean \pm S.D. An unpaired Student's *t* test was performed to test for statistical significance * *p* < 0.05; ** *p* < 0.01.

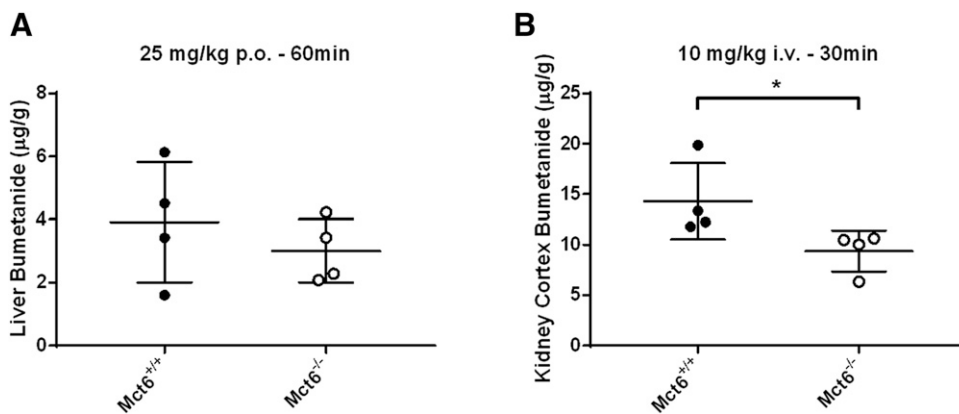


Fig. 7. Bumetanide tissue concentrations in (A) liver at 60 minutes after oral dose administration of 25 mg/kg and (B) kidney cortex at 30 minutes after intravenous dose administration of 10 mg/kg. $N = 4$ mice per group. Data are plotted as mean \pm S.D. An unpaired Student's t test was performed to test for statistical significance * $p < 0.05$.

kidney tissue concentrations, are necessary to confirm this hypothesis. Mct6 mRNA is expressed in kidney, but its protein expression and localization in the kidney (basolateral vs. brush-border membrane localization) is unknown. Further studies are necessary to elucidate the function of Mct6 in the kidney.

It is also important to note that systemic concentrations of bumetanide in humans range from nanograms per milliliter to micrograms per milliliter (Pentikainen et al., 1977; Holazo et al., 1984), similar to the range of concentrations observed in the present studies. In addition, the bioavailability and overall elimination of bumetanide is different between rodents and humans. In humans, it is reported that the bioavailability of bumetanide is approximately 80% (Holazo et al., 1984), whereas in mice we found it to be much less (~30%). This is most likely due to the rapid first-pass metabolism of bumetanide in rodents compared with humans via oxidation of the *N*-butyl side chain (Töpfer et al., 2014). In addition, the fraction eliminated unchanged in the urine in mice was calculated to be less than 25% in all cases compared with humans, which showed 60% eliminated as intact parent drug in the urine after a 1-mg oral dose of bumetanide. Because of the greater importance of renal clearance of bumetanide in humans, it is possible that human MCT6 may play a more important role in the kidney disposition and pharmacodynamics of bumetanide in humans.

In summary, this study represents the first evidence that Mct6 may play a role in moderating kidney concentrations of bumetanide in vivo, which has a downstream impact on the diuresis mediated by bumetanide. This is supported by PK/PD studies performed in our knockout animal model, as well as recent studies performed by Xu et al. (2019) that provide evidence for significant bumetanide interactions with rat Mct6. Moving forward, additional studies performed with the Mct6^{-/-} model could provide evidence for significant MCT6-mediated drug-drug interactions with other loop diuretics that could impact drug absorption, distribution, metabolism, and excretion and efficacy.

Acknowledgments

The authors would like to acknowledge M.D.P., Mark A. Bryniarski, Michael Deci, and Scott Ferguson for their assistance in animal handling.

Authorship Contributions

Participated in research design: Jones, Ruszaj, Parker, Morris.

Conducted experiments: Jones, Ruszaj.

Performed data analysis: Jones, Ruszaj, Morris.

Wrote or contributed to the writing of the manuscript: Jones, Ruszaj, Morris.

References

Blaesse P, Airaksinen MS, Rivera C, and Kaila K (2009) Cation-chloride cotransporters and neuronal function. *Neuron* 61:820–838.

- Brandt C, Nozadze M, Heuchert N, Rattka M, and Löscher W (2010) Disease-modifying effects of phenobarbital and the NKCC1 inhibitor bumetanide in the pilocarpine model of temporal lobe epilepsy. *J Neurosci* 30:8602–8612.
- Brater DC, Day B, Burdette A, and Anderson S (1984) Bumetanide and furosemide in heart failure. *Kidney Int* 26:183–189.
- Cleary RT, Sun H, Huynh T, Manning SM, Li Y, Rotenberg A, Talos DM, Kahle KT, Jackson M, Rakhade SN, et al. (2013) Bumetanide enhances phenobarbital efficacy in a rat model of hypoxic neonatal seizures [published correction appears in *PLoS One* (2013) 8]. *PLoS One* 8:e57148.
- Cook JA, Smith DE, Cornish LA, Tankanow RM, Nicklas JM, and Hyneck ML (1988) Kinetics, dynamics, and bioavailability of bumetanide in healthy subjects and patients with congestive heart failure. *Clin Pharmacol Ther* 44:487–500.
- Dixon WR, Young RL, Holazo A, Jack ML, Weinfeld RE, Alexander K, Liebman A, and Kaplan SA (1976) Bumetanide: radioimmunoassay and pharmacokinetic profile in humans. *J Pharm Sci* 65:701–704.
- Gill RK, Saksena S, Alrefai WA, Sarwar Z, Goldstein JL, Carroll RE, Ramaswamy K, and Dudeja PK (2005) Expression and membrane localization of MCT isoforms along the length of the human intestine. *Am J Physiol Cell Physiol* 289:C846–C852.
- Haas M and Forbush B III (1998) The Na-K-Cl cotransporters. *J Bioenerg Biomembr* 30:161–172.
- Han KS, Lee SH, Lee MG, and Kim ND (1993) Pharmacokinetics and pharmacodynamics of bumetanide after intravenous and oral administration to spontaneously hypertensive rats and DOCA-salt induced hypertensive rats. *Biopharm Drug Dispos* 14:533–548.
- Hasannejad H, Takeda M, Taki K, Shin HJ, Babu E, Jutabha P, Khamdang S, Aleboeyh M, Onozato ML, Tojo A, et al. (2004) Interactions of human organic anion transporters with diuretics. *J Pharmacol Exp Ther* 308:1021–1029.
- Holazo AA, Colburn WA, Gustafson JH, Young RL, and Parsonnet M (1984) Pharmacokinetics of bumetanide following intravenous, intramuscular, and oral administrations to normal subjects. *J Pharm Sci* 73:1108–1113.
- Jones RS, Parker MD, and Morris AME (2020) Monocarboxylate transporter 6-mediated interactions with prostaglandin F_{2α}: in vitro and in vivo evidence utilizing a knockout mouse model. *Pharmacometrics* 12, p 201.
- Jones RS, Parker MD, and Morris ME (2017) Quercetin, morin, luteolin, and phloretin are dietary flavonoid inhibitors of monocarboxylate transporter 6. *Mol Pharm* 14:2930–2936.
- Jones RS, Tu C, Zhang M, Qu J, and Morris ME (2019) Characterization and proteomic-transcriptomic investigation of monocarboxylate transporter 6 knockout mice: evidence of a potential role in glucose and lipid metabolism. *Mol Pharmacol* 96:364–376.
- Kahle KT, Barnett SM, Sassower KC, and Staley KJ (2009) Decreased seizure activity in a human neonate treated with bumetanide, an inhibitor of the Na(+)-K(+)-2Cl(-) cotransporter NKCC1. *J Child Neurol* 24:572–576.
- Kim EJ and Lee MG (2001) Pharmacokinetics and pharmacodynamics of intravenous bumetanide in mutant Nagase analbuminemic rats: importance of globulin binding for the pharmacodynamic effects. *Biopharm Drug Dispos* 22:147–156.
- Kobayashi Y, Ohshiro N, Sakai R, Ohbayashi M, Kohyama N, and Yamamoto T (2005) Transport mechanism and substrate specificity of human organic anion transporter 2 (hOat2 [SLC22A7]). *J Pharm Pharmacol* 57:573–578.
- Kohyama N, Shiokawa H, Ohbayashi M, Kobayashi Y, and Yamamoto T (2013) Characterization of monocarboxylate transporter 6: expression in human intestine and transport of the antidiabetic drug nateglinide. *Drug Metab Dispos* 41:1883–1887.
- Lee SH, Lee MG, and Kim ND (1994) Pharmacokinetics and pharmacodynamics of bumetanide after intravenous and oral administration to rats: absorption from various GI segments. *J Pharmacokinet Biopharm* 22:1–17.
- Levine DZ, Iacovitti M, Robertson SJ, and Mokhtar GA (2006) Modulation of single-nephron GFR in the db/db mouse model of type 2 diabetes mellitus. *Am J Physiol Regul Integr Comp Physiol* 290:R975–R981.
- Lytle C, Xu JC, Biemesderfer D, and Forbush B III (1995) Distribution and diversity of Na-K-Cl cotransport proteins: a study with monoclonal antibodies. *Am J Physiol* 269:C1496–C1505.
- Mao S, Garzon-Muvdi T, Di Fulvio M, Chen Y, Delpire E, Alvarez FJ, and Alvarez-Leefmans FJ (2012) Molecular and functional expression of cation-chloride cotransporters in dorsal root ganglion neurons during postnatal maturation. *J Neurophysiol* 108:834–852.
- Murakami Y, Kohyama N, Kobayashi Y, Ohbayashi M, Ohtani H, Sawada Y, and Yamamoto T (2005) Functional characterization of human monocarboxylate transporter 6 (SLC16A5). *Drug Metab Dispos* 33:1845–1851.
- Musa-Aziz R, Boron WF, and Parker MD (2010) Using fluorometry and ion-sensitive micro-electrodes to study the functional expression of heterologously-expressed ion channels and transporters in *Xenopus* oocytes. *Methods* 51:134–145.
- Pentikäinen PJ, Penttilä A, Neuvonen PJ, and Gothoni G (1977) Fate of [¹⁴C]-bumetanide in man. *Br J Clin Pharmacol* 4:39–44.
- Puskarjov M, Kahle KT, Ruusuvoori E, and Kaila K (2014) Pharmacotherapeutic targeting of cation-chloride cotransporters in neonatal seizures. *Epilepsia* 55:806–818.

- Römermann K, Fedrowitz M, Hampel P, Kaczmarek E, Töllner K, Erker T, Sweet DH, and Löscher W (2017) Multiple blood-brain barrier transport mechanisms limit bumetanide accumulation, and therapeutic potential, in the mammalian brain. *Neuropharmacology* **117**: 182–194.
- Smith DE and Lau HS (1983) Determinants of bumetanide response in the dog: effect of probenecid. *J Pharmacokinetic Biopharm* **11**:31–46.
- Töllner K, Brandt C, Römermann K, and Löscher W (2015) The organic anion transport inhibitor probenecid increases brain concentrations of the NKCC1 inhibitor bumetanide. *Eur J Pharmacol* **746**:167–173.
- Töpfer M, Töllner K, Brandt C, Twele F, Bröer S, and Löscher W (2014) Consequences of inhibition of bumetanide metabolism in rodents on brain penetration and effects of bumetanide in chronic models of epilepsy. *Eur J Neurosci* **39**:673–687.
- Walmsley L (1985) *Pharmacokinetics of Bumetanide, Lorazepam and Clofibrac Acid in Cynomolgus Monkeys and Baboons*, Loughborough University of Technology.
- Weaver ML, Orwig BA, Rodriguez LC, Graham ED, Chin JA, Shapiro MJ, McLeod JF, and Mangold JB (2001) Pharmacokinetics and metabolism of nateglinide in humans. *Drug Metab Dispos* **29**:415–421.
- Xu F, Zhu L, Qian C, Zhou J, Geng D, Li P, Xuan W, Wu F, Zhao K, Kong W, et al. (2019) Impairment of intestinal monocarboxylate transporter 6 function and expression in diabetic rats induced by combination of high-fat diet and low dose of streptozocin: involvement of butyrate-peroxisome proliferator-activated receptor- γ activation. *Drug Metab Dispos* **47**:556–566.

Address correspondence to: Dr. Marilyn E. Morris, Department of Pharmaceutical Sciences, University at Buffalo, State University of New York, 304 Pharmacy Bldg., Buffalo, NY 14214. E-mail: memorris@buffalo.edu
